Kaluza-Klein FRW Tsallis holographic dark energy model in scalar-tensor theory of gravitation

K. Dasunaidu[1,a], Y. Aditya[1,b], V. Sreenivasa Rao[2,3]
[1] Department of Mathematics, GMR Institute of Technology, Rajam-532127, India
[2] Department of Mathematics, Sri G.C.S.R. College, Rajam-532127, India
[3] Department of Mathematics, GIET University, Gunupur-765002, India
[a] dasunaidu.k@gmrit.edu.in, [b] aditya.y@gmrit.edu.in
(Submitted on 08 December 2022; Accepted on 30 April 2023)

Abstract. This paper aims to investigate the dynamical behaviour of Kaluza-Klein (KK) FRW type dark energy cosmological models in the context of Saez and Ballester's scalar-tensor theory of gravitation (Phys. Lett. A113, 467:1986). In this theory, the Tsallis holographic dark energy model is provided by solving the field equations with variable deceleration parameter proposed by Mishra et al. (Int. J. Theor. Phys. 2016; **55:** 1241). The equation of state parameter (ω_{de}), the deceleration parameter (q(t)), statefinder parameter (r,s), $\omega_{de} - \omega'_{de}$ plane, squared speed of sound, and energy conditions have all been studied for our models. We investigated their dynamic behaviour using graphical representation and Planck Collaboration data. It has been discovered that our models describe the accelerated expansion of the universe and that our theoretical results are reasonably consistent with the observational data.
Key words: Kaluza-Klein model; Saez-Ballester theory; Scalar-tensor theory; Tsallis holographic dark energy model.

1 Introduction

Experiment data from Supernova Ia have confirmed that the universe is currently accelerating (Riess et al. 1998; Perlmutter et al. 1999). It has also been proposed that the primary cause of this is an exotic negative pressure known as 'dark energy.' Even today, this is a cosmological mystery. Two approaches are being actively considered in the literature to explain the accelerated expansion of the universe. One approach is to build dark energy models and study their dynamics. Another approach is to modify Einstein's theory of gravitation, determine the cosmological models in the modified theories of gravity, and then investigate their dynamical aspects. The cosmological constant is the most straightforward candidate for dark energy. However, it is plagued by coincidence and other issues. As a result, other DE candidates such as quintessence, phantom, k- essence and quintom models have also been considered to explain DE (Ratra and Peebles 1988; Chiba et al. 2000; Elizalde et al. 2004; Caldwell 2002). Among the different dynamical DE models, the HDE model, in particular, has been a prominent model for examining the DE mystery in recent years. It was based on the quantum properties of black holes (BH), which have been widely studied in the literature to investigate quantum gravity (Li 2004; Susskind 1995). Due to the formation of BH in quantum field theory, the holographic principle states that the bound on the vacuum energy Λ of a system with size L should not cross the limit of the BH mass of the same size. The following is the definition of HDE's energy density (Cohen et al. 1999)

$$\rho_{de} = 3d^2 m_p^2 \, (L)^{-2} \tag{1}$$

The reduced Planck mass is mp, the numerical constant is $3d^2$, and the IR cutoff is L. Several entropy formalisms have been used to develop and evaluate

cosmological models in recent years. Tsallis HDE (THDE) is one of the new HDE models developed and is never stable at the classical level (Tavayef et al. 2018; Tsallis et al. 2013). Several investigations on THDE models in alternative theories of gravitation have been done by several researchers all over the globe (Aditya et al. 2019; Ghaffari et al. 2019; Maity et al. 2019; Iqbal et al. 2019; Santhi and Sobhanbabu 2020).

For this purpose, we are interested in the "modified gravity" approach. The f(R) and f(R,T) theories of gravity (Nojiri et al. 2005; Harko et al. 2011) (R is the scalar curvature and T is the trace of the energy-momentum tensor), Brans-Dicke (BD) and Saez-Ballester (SB) scalar-tensor theories of gravitation (Brans and Dicke 1961; Saez and Ballester 1986) are significant modifications of Einstein's theory of gravitation. As a result, several investigations of DE cosmological models have been conducted in the above alternative theories of gravitation to explain DE models by studying their dynamical aspects. The researchers focused on anisotropic Bianchi type DE models in the majority of the above cases. Many authors (Aditya 2023; Aditya et al. 2023; Rao et al. 2015a, 2015b; Aditya et al. 2016; Rao et al. 2018; Aditya and Reddy 2018a, 2018b, 2018c; Aditya and Reddy 2019; Rao et al. 2012; Dasunaidu et al. 2018a, 2018b; Ravindranath et al. 2018; Prasanthi and Aditya 2019, 2021; Aditya et al. 2019; Santhi et al. 2016a, 2016b, 2017; Deniel Raju et al. 2020; Rao et al. 2022) have recently discussed several DE models in modified theories of gravitation.

We are mainly interested in Saez and Ballester's scalar-tensor theory of gravity (Saez 1986). In addition to a metric tensor field, a scalar field φ has been introduced in BD theory to serve as the inverse of the gravitational constant. This was done to incorporate Mach's principle more thoroughly. Later, Saez and Ballester developed a new scalar-tensor theory of gravitation in which the metric of space-time is simply coupled with a dimensionless scalar field. However, an antigravity regime exists in this theory. This theory contributes to the solution of the "missing mass" problem in non-flat FRW cosmologies. The gravitational action is regarded as

$$I = \int_{\Sigma} (L + GL_m)\sqrt{-g}\; dx\; dy\; dz\; dt$$

where L_m denotes the matter Lagrangian. The SB scalar-tensor theory field equations result from a variation of the gravitational action principle $\delta I = 0$.

$$R_{ij} - \frac{1}{2}g_{ij}R - w\varphi^n\left(\varphi_{,i}\varphi_{,j} - \frac{1}{2}g\varphi_{,k}\varphi^{,k}\right) = -T \tag{2}$$

Here the scalar field φ satisfies the equation

$$2\varphi^n\varphi'^{i}_{ji} + n\varphi^{n-1}\varphi_{,k}\varphi'^{k} = 0 \tag{3}$$

where R_{ij} is the Ricci tensor, R is the Ricci scalar, w is a dimensionless constant, T is the energy-momentum tensor of matter (The relativistic units, $8\pi G = c = 1$ are used here).

Also, we have the energy conservation equation as

$$T^{ij}{}_{;j} = 0. \tag{4}$$

Higher-dimensional space-time research is still required, to integrate gravity with other gauge interactions. Extra dimensions are important in cosmology, especially at the early stages of the universe. The universe's current four-dimensional stage may have been preceded by a multidimensional stage, according to theory. As time passes, the standard dimensions grow while the extra dimensions shrink to Planckian dimensions, which are beyond our current experimental capabilities to detect. This discovery has piqued the interest of many scholars who want to learn more about cosmological theories in the domain of higher dimensions. This extra dimension was employed by Kaluza and Klein to unify gravity and electromagnetism in a five-dimensional general relativity theory.

Due to dynamical contraction as time passes in Kaluza-Klein's theories, the extra dimensions are not visible (Chodos and Detweller 1980). It is thought that during the early phases of the universe's evolution, the cosmos may have experienced a higher dimensional era (Witten 1984; Applequist and Chodos 1983). In addition, as time passes, the universe compacts and shrinks to four dimensions. DE models with a scalar field play a crucial role in the discussion of the universe's early stages of evolution. Several authors have looked into DE models in five dimensions in BD theory and SB theory. In BD theory, Reddy et al. (2016) presented the five-dimensional minimally interacting holographic DE model. Non-compact FRW type KK cosmological models were examined by Ozel et al. (2010) and Sharif and Khanum (2011). In the BD theory of gravity, Aditya and Reddy (2018) studied FRW type KK modified holographic Ricci DE models. Naidu et al. (2021) have explored Kaluza-Klein FRW dark energy models in modified theories of gravitation. As a result, KK scalar-tensor models have become extremely important.

In this paper, we obtain a new class of Tsallis HDE cosmological models in FRW type KK space-time in the SB theory of gravitation. The plan of this paper is the following: In Section 2 we obtain the field equations of SB theory with the help of FRW type KK metric in the presence of a Tsallis HDE fluid. Section 3 is devoted to the solutions of the field equations and their corresponding model. In Section 4 we investigate the cosmological parameters of each of the models and discuss their physical significance. The last section involves a summary and some conclusions.

2 Field Equations

We propose to use the FRW type KK metric to get the explicit field equations of SB theory

$$ds^2 = dt^2 - a^2(t)\left[\frac{dr^2}{1-kr^2} + r^2(d\theta^2 + sin^2\theta d\phi^2) + (1-kr^2)d\psi^2\right] \tag{5}$$

where $a(t)$ is the five-dimensional average scale factor of the model and $k = 0$, 1, -1 represents the curvature parameter for a flat, closed and open universe.

The energy-momentum tensors for DE fluid ($T_{ij}^{(de)}$) and pressure-less matter ($T_{ij}^{(m)}$) are given by

$$T_{ij}^{(de)} = (\rho_{de} + p_{de})u^i u_j - p_{de} g_{ij}; \quad T_{ij}^{(m)} = \rho_m u_i u_j \tag{6}$$

where ρ_{de} is DE density, p_{de} is DE pressure, ρ_m the energy density of matter and

$$u^i u_i = 1, \; u^i u_j = 0. \tag{7}$$

Now the field equations (2) take the form

$$R_{ij} - \frac{1}{2} g_{ij} R - w\varphi^n \left(\varphi_{,i}\varphi_{,j} - g_{ij}\varphi_{,k}\varphi^{,k} \right) = -T_{ij}^{(de)} - T_{ij}^{(m)} \tag{8}$$

where $T_{ij}^{(de)}$and $T_{ij}^{(m)}$ are given by Eq. (6).

Now, field Eqs. (8), (3) and (4) with the help of Eqs. (6) and (7) for the metric (5) can be written as

$$6\frac{\dot{a}^2}{a^2} + \frac{6k}{a^2} + \frac{w}{2}\varphi^n \dot{\varphi}^2 = \rho_m + \rho_{de} \tag{9}$$

$$3\left(\frac{\ddot{a}}{a} + \frac{\dot{a}^2}{a^2} + \frac{k}{a^2} \right) - \frac{w}{2}\varphi^n \dot{\varphi}^2 = -\omega_{de}\rho_{de} \tag{10}$$

$$\ddot{\varphi} + 4\,\dot{\varphi}\frac{\dot{a}}{a} + \frac{n}{2}\frac{\dot{\varphi}^2}{\varphi} = 0 \tag{11}$$

$$\rho_{de} + \rho_m + 4\frac{\dot{a}}{a}[\rho_m + (1 + \omega_{de})\,\rho_{de}] = 0 \tag{12}$$

where $\omega_{de} = \frac{p_{de}}{\rho_{de}}$ is the equation of state (EoS) parameter of DE and an overhead dot indicates differentiation with respect to time t.

3 Solutions and the models

We can see that Eqs. (9) – (12) are three independent equations in five unknowns $a(t)$, φ, ρ_m, ρ_{de} and ω_{de}. As a result, two more conditions are required to obtain a determinate solution. Also, the early decelerated phase of the universe is represented by a positive value of the deceleration parameter, whereas the accelerated phase is represented by a negative number. Our universe is expanding at an accelerated rate, according to recent cosmological findings. By modifying its signature, the deceleration parameter must move smoothly from early deceleration to present increasing expansion. As a result, the deceleration parameter must be time-varying rather than constant. To discover the corresponding cosmological models of the universe, we use the following form of average scale factor, which provides us with a time-dependent deceleration

parameter. Mishra et al. (2016) proposed a new ansatz for the average scale factor, which is given by

$$a\,(t) = [sinh\,(\alpha t)]^{\frac{1}{\beta}} \tag{13}$$

which provides a time-dependent deceleration parameter. Now from Eqs. (11) and (13) we get the scalar field as

$$\varphi(t) = \left(\frac{(n+2)\,\varphi_0\ \beta}{2\ \alpha\ \ (\beta-4)}(sinh\,(\alpha\ t))^{\frac{\beta-4}{\beta}}\right)^{\frac{2}{n+2}} \tag{14}$$

where ϕ_0 is a constant of integration. Using Eq. (13) in metric (5) we get the model as

$$ds^2 = dt^2 - [sinh\,(\alpha t)]^{\frac{2}{\beta}}\left[dr^2 + r^2(d\theta^2 + sin^2\theta d\phi^2) + d\psi^2\right] \tag{15}$$

4 Physical discussion of the models

In this section, we examine each model's important cosmological parameters and describe their physical significance in cosmology.

The spatial volume in the model is

$$V = a^4(t) = [sinh\,(\alpha t)]^{\frac{4}{\beta}} \tag{16}$$

The average Hubble parameter ($H(t)$) and scalar expansion ($\theta(t)$) are

$$H = \frac{\theta}{4} = \frac{\dot{a}}{a} = \frac{\alpha}{\beta}coth(\alpha t) \tag{17}$$

Here we assume Tsallis holographic dark energy with Granda-Oliveros cut-off as the suitable candidate for dynamical dark energy. Its energy density is defined as follows (Tsallis and Cirto 2013)

$$\rho_{de} = 3d^2(L)^{2\ \delta-4}$$

where d is an unknown parameter. By assuming the Hubble horizon as the IR cutoff, $L = H^{-1}$, the energy density of THDE takes the form

$$\rho_{de} = 3d^2(H)^{-2\ \delta+4}$$

From Eq. (17) we obtain the THDE density of our model obtained as

$$\rho_{de} = 3d^2\left(\frac{\alpha\ coth\,(\alpha\ t)}{\beta}\right)^{-2\ \delta+4} \tag{18}$$

and from Eqs. (9), (13), (14) and (18) we get the energy density of matter as

$$\rho_m = \frac{6\alpha^2(cosh\,(\alpha\ t))^2}{\beta^2(sinh\,(\alpha\ t))^2} + \frac{w\varphi_0}{2\Big((sinh\,(\alpha\ t))^{\beta-1}\Big)^4} - 3d^2\left(\frac{\alpha\ cosh\,(\alpha\ t)}{\beta\ sinh\,(\alpha\ t)}\right)^{-2\ \delta+4} \tag{19}$$

Scalar field:

Figure 1 describes the behaviour of a scalar field over cosmic time for various values of the parameter n, which has an important influence in its evolution. For all values of n, we notice that the scalar field reduces with cosmic time. The scalar field, on the other hand, grows in sync with the value n. We see that the scalar field is decreasing and that the kinetic energy is increasing as a result. This tendency is quite identical to the scalar field in the dark energy scalar field models developed by Jawad et al. (2015), Raju et al. (2019) and Bhaskara Rao et al. (2022).

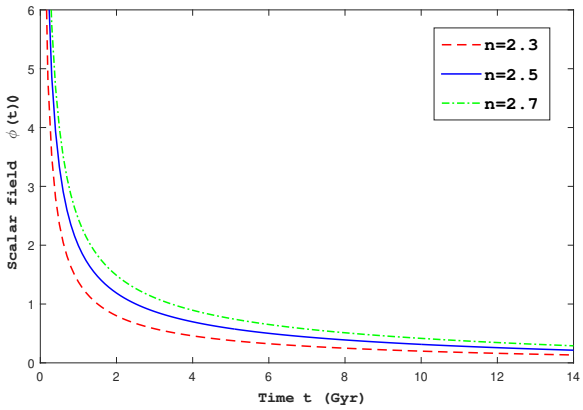

Fig. 1. Plot of scalar field versus cosmic time t for $\beta = 1.5$, $\alpha = 0.11$, $n = 2.3, w = 0.0075$, $d = 0.38$, $\delta = 1.5$ and $\varphi_0 = 0.5$.

Deceleration parameter:

The deceleration parameter (DP) is often used to evaluate how rapidly the universe is expanding. It's expressed as

$$q = -1 - \frac{\dot{H}}{H^2}. \tag{20}$$

Making use of DP's signature the nature of the universe's expansion is explained. Positive values of DP show a deceleration phase, whereas $-1 \leq q < 0$ shows an accelerated expansion phase. The deceleration parameter of our model is

$$q = \beta(sech(\alpha t))^2 - 1\,. \tag{21}$$

Figure 2 illustrates the behaviour of DP in terms of cosmic time t for our model. This indicates a significant transition from positive to negative. As a result, our model has a smooth transition from the early deceleration epoch

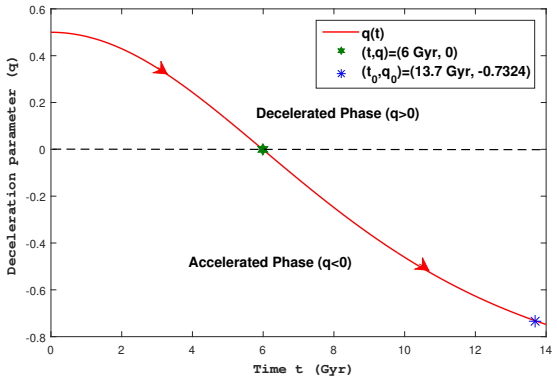

Fig. 2. Plot of deceleration parameter versus time t for $\beta = 1.5$ and $\alpha = 0.11$.

to the universe's current acceleration era. The present value of the DP seems to be -0.7324 and our model starts accelerating expansion at ts 6 Gyr, or 7.7 Gyr ago from today ($t_0 = 13.7$ Gyr). This behaviour is supported by data from a variety of observational schemes (Cunha 2009; Li et al. 2011; Amirhashchi and Amirhashchi 2019; Capozziello et al. 2019).

Energy conditions:

For our THDE model, we discuss the well-known energy conditions. The Raychaudhuri equations, which have an important significance in any discussion of the congruence of null and time-like geodesics, gave rise to the study of energy conditions. The energy conditions are also used to show several general theorems regarding how powerful gravitational fields operate. The following are the standard energy conditions:

– Null energy conditions (NEC): $\rho_{de} + p_{de} \geq 0$,
– Weak energy conditions (WEC): $\rho_{de} \geq 0$, $\rho_{de} + p_{de} \geq 0$,
– Strong energy conditions (SEC): $\rho_{de} + p_{de} \geq 0$, $\rho_{de} + 3p_{de} \geq 0$,
– Dominant energy condition (DEC): $\rho_{de} \geq 0$, $\rho_{de} \pm p_{de} \geq 0$.

According to the NEC, the universe's energy density decreases as it expands, and its violation could lead to the Big Rip in cosmology. The violation of the SEC condition represents the universe's rapid expansion. The Hawking-Penrose singularity theorems demonstrate the validity of SEC and WEC. Because their failure causes other energy conditions to be violated, the WEC and NEC are essential among all energy conditions. Figure 3 depicts the energy conditions for various values of 'n' in our model. The SEC is observed to be satisfied at the beginning of the period and then violated subsequently. As a result, the model causes the universe to expand at a faster rate. Furthermore, as should be the case, our model violates the SEC. Throughout the evolution of the universe, all other energy conditions are fulfilled. Also, it can be seen that the energy conditions are almost the same for all the values of parameter 'n', i.e., the energy conditions are independent of the scalar field. This

is attributed to the universe's late-time acceleration, which is supported by current observational data.

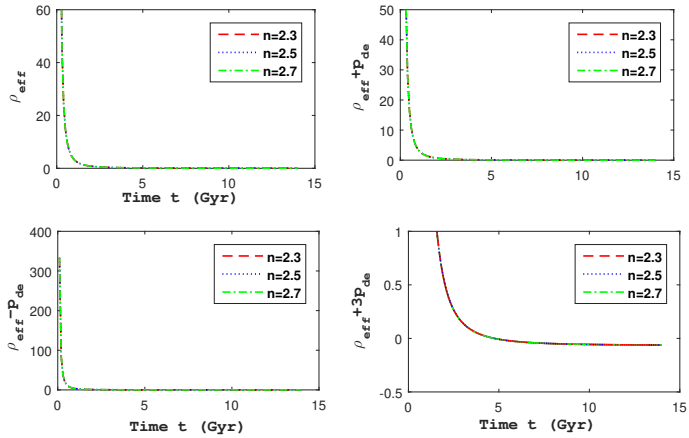

Fig. 3. Plot of energy conditions versus cosmic time t for $\beta = 1.5,\ \alpha = 0.11,\ n = 2.3,\ w = 0.0075,\ d = 0.38,\ \delta = 1.5\ and\ \varphi_0 = 0.5.$

EoS parameter:

The EoS parameter (ω) is used to categorise the different stages of the expanding universe. It calculates the cosmological constant/vacuum era for $\omega = -1$, the quintessence for $-1 < \omega < \frac{-1}{3}$, the phantom era for $\omega < -1$, and the quintom era for both $\omega > -1$ and $\omega < -1$. From Eqs. (10), (13), (14) and (18) we have the EoS parameter as

$$\omega_{de} = -\frac{1}{3d^2}\left\{\frac{3}{(sinh(\alpha\ \ t))^{\beta^{-1}}}\left\{\frac{(sinh(\alpha\ t))^{\beta^{-1}}\alpha^2(cosh(\alpha\ t))^2}{\beta^2(sinh(\alpha\ t))^2} + \frac{(sinh(\alpha\ t))^{\beta^{-1}}\alpha^2}{\beta}\right.\right.$$
$$\left.\left. - \frac{(sinh(\alpha\ t))^{\beta^{-1}}\alpha^2(cosh(\alpha\ t))^2}{\beta\ (sinh(\alpha\ t))^2}\right\} + \frac{3\alpha^2(cosh(\alpha\ t))^2}{\beta^2(sinh(\alpha\ t))^2}\right.$$
$$\left. - \frac{w\phi_0}{2\left((sinh(\alpha\ t))^{\beta^{-1}}\right)^4}\right\}\left(\left(\frac{\alpha\ cosh(\alpha\ t)}{\beta\ sinh(\alpha\ t)}\right)^{2\ \delta-4}\right) \tag{22}$$

According to Fig. 4, the EoS parameter begins in the matter-dominated era, evolves to the quintessence DE era, and finally approaches the vacuum DE and phantom era for different values of δ= 1.4, 1.45, and 1.5. The figure clearly shows that for $\delta = 1.5$, the EoS parameter becomes -1, i.e., the cosmological constant. This is in agreement with the predictions of Saridakis et al. (2018). It is also worth noting that for δ=1.45 and 1.5, the universe model crosses the phantom divided line (PDL) $\omega_{de} = -1$ and enters the phantom region. The

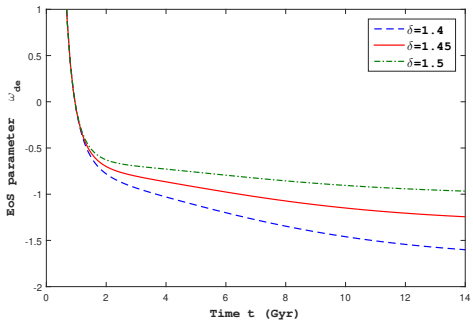

Fig. 4. Plot of EoS parameter versus time t for $\beta = 1.5,\ \alpha = 0.11,\ n = 2.3,\ w = 0.0075,\ d = 0.38,\ \delta = 1.5$ *and* $\varphi_0 = 0.5$.

current values of our model's EoS parameters (δ, ω_{de})=(1.4, -1.59), (1.45, -1.24), and (1.5, -0.96) are in good agreement with Planck observational data (Aghanim et al. 2018).

Squared sound speed:

The squared sound speed parameter facilitates the exploration of the stability of DE models depending on the sign of v_s^2. The model's stability is determined by the positive sign of v_s^2, whereas the model's instability is determined by the negative sign of v_s^2. It is defined as:

$$v_s^2 = \frac{\dot{p}_{de}}{\dot{\rho}_{de}} = \omega_{de} + \frac{\rho_{de}}{\dot{\rho}_{de}}\dot{\omega}_{de}. \tag{23}$$

$$\begin{aligned} v_s^2 = {} & \frac{\alpha\ cosh\,(\alpha\ t)}{(-2\ \delta+4)\,\beta\ sinh\,(\alpha\ t)}\left\{\frac{(-2\ \delta+4)\quad \beta\ sinh\,(\alpha\ t)}{3d^2\alpha\ cosh\,(\alpha\ t)}\left\{\frac{3}{(sinh\,(\alpha t))^{\beta-1}}\right.\right. \\ & \times\left\{\frac{(sinh\,(\alpha\ t))^{\beta-1}\alpha^2(cosh\,(\alpha\ t))^2}{\beta^2(sinh\,(\alpha\ t))^2} - \frac{(sinh\,(\alpha\ t))^{\beta-1}\alpha^2(cosh\,(\alpha\ t))^2}{\beta\ (sinh\,(\alpha\ t))^2}\right. \\ & \left.\left.+\frac{(sinh\,(\alpha\ t))^{\beta-1}\alpha^2}{\beta}\right\} + 3\frac{\alpha^2(cosh\,(\alpha\ t))^2}{\beta^2(sinh\,(\alpha\ t))^2} - \frac{w\phi_0}{2\Big((sinh\,(\alpha\ t))^{\beta-1}\Big)^4}\right\} \\ & \left(\frac{\alpha^2}{\beta} - \frac{\alpha^2(cosh\,(\alpha\ t))^2}{\beta\ (sinh\,(\alpha\ t))^2}\right)\left(\left(\frac{\alpha\ cosh\,(\alpha\ t)}{\beta\ sinh\,(\alpha\ t)}\right)^{-2\ \delta+4}\right)^{-1} \\ & - \frac{1}{3d^2}\left\{\frac{3}{(sinh\,(\alpha\ t))^{\beta-1}}\left\{\frac{(sinh\,(\alpha\ t))^{\beta-1}\alpha^3(cosh\,(\alpha\ t))^3}{\beta^3(sinh\,(\alpha\ t))^3}\right.\right. \\ & +3\frac{(sinh\,(\alpha\ t))^{\beta-1}\alpha^3 cosh\,(\alpha\ t)}{\beta^2 sinh\,(\alpha\ t)} - 3\frac{(sinh\,(\alpha\ t))^{\beta-1}\alpha^3(cosh\,(\alpha\ t))^3}{\beta^2(sinh\,(\alpha\ t))^3} \\ & \left.\left.-2\frac{(sinh\,(\alpha\ t))^{\beta-1}\alpha^3 cosh\,(\alpha\ t)}{\beta\ sinh\,(\alpha\ t)} + 2\frac{(sinh\,(\alpha\ t))^{\beta-1}\alpha^3(cosh\,(\alpha\ t))^3}{\beta\ (sinh\,(\alpha\ t))^3}\right\}\right. \end{aligned}$$

$$-\frac{3\alpha\ cosh\,(\alpha\ t)}{(sinh\,(\alpha\ t))^{\beta-1}\beta\ sinh\,(\alpha\ t)}\left\{\frac{(sinh\,(\alpha\ t))^{\beta-1}\alpha^2(cosh\,(\alpha\ t))^2}{\beta^2(sinh\,(\alpha\ t))^2}+\frac{(sinh\,(\alpha\ t))^{\beta-1}\alpha^2}{\beta}\right.$$
$$\left.-\frac{(sinh\,(\alpha\ t))^{\beta-1}\alpha^2(cosh\,(\alpha\ t))^2}{\beta\ (sinh\,(\alpha\ t))^2}\right\}\ +6\frac{\alpha^3 cosh\,(\alpha\ t)}{\beta^2 sinh\,(\alpha\ t)}-6\frac{\alpha^3(cosh\,(\alpha\ t))^3}{\beta^2(sinh\,(\alpha\ t))^3}$$
$$+\frac{2w\phi_0\ \alpha\ cosh\,(\alpha\ t)}{\left((sinh\,(\alpha\ t))^{\beta-1}\right)^4\beta\ sinh\,(\alpha\ t)}\left\{\left(\left(\frac{\alpha\ cosh\,(\alpha\ t)}{\beta\ sinh\,(\alpha\ t)}\right)^{2\ \delta-4}\right)\right\}$$
$$\times\left(\frac{\alpha^2}{\beta}-\frac{\alpha^2(cosh\,(\alpha\ t))^2}{\beta\ (sinh\,(\alpha\ t))^2}\right)^{-1}-\frac{1}{3d^2}\left\{\frac{3}{(sinh\,(\alpha\ t))^{\beta-1}}\left\{\frac{(sinh\,(\alpha\ t))^{\beta-1}\alpha^2}{\beta^2(tanh\,(\alpha\ t))^2}\right.\right.$$
$$\left.+\frac{(sinh\,(\alpha\ t))^{\beta-1}\alpha^2}{\beta}-\frac{(sinh\,(\alpha\ t))^{\beta-1}\alpha^2(cosh\,(\alpha\ t))^2}{\beta\ (sinh\,(\alpha\ t))^2}\right\}+\frac{3\alpha^2(cosh\,(\alpha\ t))^2}{\beta^2(sinh\,(\alpha\ t))^2}$$
$$\left.-\frac{w\phi_0}{2\left((sinh\,(\alpha\ t))^{\beta-1}\right)^4}\right\}\left(\left(\frac{\alpha\ cosh\,(\alpha\ t)}{\beta\ sinh\,(\alpha\ t)}\right)^{2\ \delta-4}\right) \tag{24}$$

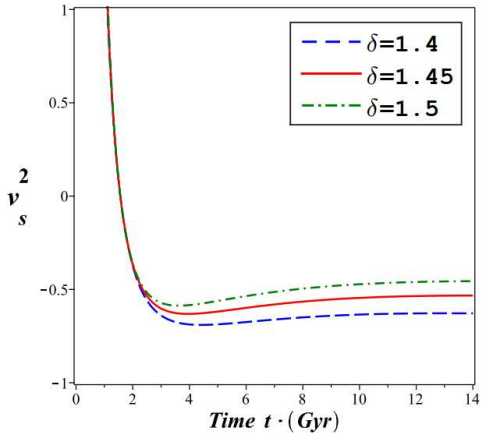

Fig. 5. Plot of v_s^2 versus time t for $\beta = 1.5,\ \alpha = 0.11,\ n = 2.3,\ w = 0.0075,\ d = 0.38,\ \delta = 1.5$ *and* $\varphi_0 = 0.5$.

We can calculate the squared speed of sound by substituting expressions for the parameters in Eq. (26). We numerically investigated the behaviour of squared sound speed v_s^2 by plotting it in terms of time t, as shown in Fig. 5. It can be seen that v_s^2 exhibits the model's stable behaviour early on, but the model becomes unstable later on.

$\omega_{de} - \omega'_{de}$:

Caldwell and Linder (2005) proposed the $\omega_{de} - \omega'_{de}$ plane (where prime signifies the derivative of 'ln(a(t))') to investigate the DE model's cosmic evolution.

They hypothesized that the $\omega_{de}-\omega'_{de}$ plane can be divided into two regions: freezing ($\omega_{de}<0$, $\omega'_{de}<0$) and thawing ($\omega_{de}<0$, $\omega'_{de}>0$) regions.

$$\omega'_{de}=\frac{\beta\ sinh\left(\alpha\ t\right)}{\alpha\ cosh\left(\alpha\ t\right)}\Bigg\{\frac{(-2\ \delta+4)\quad\beta\ sinh\left(\alpha\ t\right)}{3d^2\alpha\ cosh\left(\alpha\ t\right)}\Bigg\{\frac{3}{\left(sinh\left(\alpha t\right)\right)^{\beta^{-1}}}\times\Bigg\{\frac{\left(sinh\left(\alpha\ t\right)\right)^{\beta^{-1}}\alpha^2}{\beta}$$
$$\frac{\left(sinh\left(\alpha\ t\right)\right)^{\beta^{-1}}\alpha^2(cosh\left(\alpha\ t\right))^2}{\beta^2(sinh\left(\alpha\ t\right))^2}-\frac{\left(sinh\left(\alpha\ t\right)\right)^{\beta^{-1}}\alpha^2(cosh\left(\alpha\ t\right))^2}{\beta\ \left(sinh\left(\alpha\ t\right)\right)^2}\Bigg\}$$
$$+3\frac{\alpha^2(cosh\left(\alpha\ t\right))^2}{\beta^2(sinh\left(\alpha\ t\right))^2}-\frac{w\phi_0}{2\left(\left(sinh\left(\alpha\ t\right)\right)^{4\beta^{-1}}\right)}\Bigg\}\left(\frac{\alpha^2}{\beta}-\frac{\alpha^2(cosh\left(\alpha\ t\right))^2}{\beta\ \left(sinh\left(\alpha\ t\right)\right)^2}\right)$$
$$\times\left(\left(\frac{\alpha\ cosh\left(\alpha\ t\right)}{\beta\ sinh\left(\alpha\ t\right)}\right)^{2\ \delta-4}\right)-\frac{1}{3d^2}\Bigg\{\frac{3}{\left(sinh\left(\alpha\ t\right)\right)^{\beta^{-1}}}\Bigg\{\frac{\left(sinh\left(\alpha\ t\right)\right)^{\beta^{-1}}\alpha^3(cosh\left(\alpha\ t\right))^3}{\beta^3(sinh\left(\alpha\ t\right))^3}$$
$$+3\frac{\left(sinh\left(\alpha\ t\right)\right)^{\beta^{-1}}\alpha^3cosh\left(\alpha\ t\right)}{\beta^2sinh\left(\alpha\ t\right)}\quad-3\frac{\left(sinh\left(\alpha\ t\right)\right)^{\beta^{-1}}\alpha^3(cosh\left(\alpha\ t\right))^3}{\beta^2(sinh\left(\alpha\ t\right))^3}$$
$$-2\frac{\left(sinh\left(\alpha\ t\right)\right)^{\beta^{-1}}\alpha^3cosh\left(\alpha\ t\right)}{\beta\ sinh\left(\alpha\ t\right)}\quad+2\frac{\left(sinh\left(\alpha\ t\right)\right)^{\beta^{-1}}\alpha^3(cosh\left(\alpha\ t\right))^3}{\beta\ \left(sinh\left(\alpha\ t\right)\right)^3}\Bigg\}$$
$$-\frac{3\alpha\ cosh\left(\alpha\ t\right)}{\left(sinh\left(\alpha\ t\right)\right)^{\beta^{-1}}\beta\ sinh\left(\alpha\ t\right)}\Bigg\{\frac{\left(sinh\left(\alpha\ t\right)\right)^{\beta^{-1}}\alpha^2(cosh\left(\alpha\ t\right))^2}{\beta^2(sinh\left(\alpha\ t\right))^2}+\frac{\left(sinh\left(\alpha\ t\right)\right)^{\beta^{-1}}\alpha^2}{\beta}$$
$$-\frac{\left(sinh\left(\alpha\ t\right)\right)^{\beta^{-1}}\alpha^2(cosh\left(\alpha\ t\right))^2}{\beta\ \left(sinh\left(\alpha\ t\right)\right)^2}\Bigg\}+6\frac{\alpha^3cosh\left(\alpha\ t\right)}{\beta^2sinh\left(\alpha\ t\right)}-6\frac{\alpha^3(cosh\left(\alpha\ t\right))^3}{\beta^2(sinh\left(\alpha\ t\right))^3}$$
$$+2\frac{w\phi_0\ \alpha\ cosh\left(\alpha\ t\right)}{\left(\left(sinh\left(\alpha\ t\right)\right)^{\beta^{-1}}\right)^4\beta\ sinh\left(\alpha\ t\right)}\Bigg\}\left(\left(\frac{\alpha\ cosh\left(\alpha\ t\right)}{\beta\ sinh\left(\alpha\ t\right)}\right)^{-2\ \delta+4}\right)^{-1}\Bigg\}\tag{25}$$

Figure 6 depicts the development of $\omega_{de}-\omega'_{de}$ plane of our model. We have noticed that $\omega_{de}-\omega'_{de}$ plane represents the freezing region throughout the evolution of the universe. The $\omega_{de}-\omega'_{de}$ plane of our model is consistent with recent observations, as the freezing zone has a faster rate of cosmic expansion than the thawing region.

Statefinder parameters:

The dynamics of the universe's expansion can be explained using Hubble and deceleration parameters. However, in the modern scenario, all dynamical DE models have the same values for these cosmological parameters. As a result, these parameters failed to identify the best-fitting dynamical DE model among a variety of models. With this goal in mind, Sahni et al. (2003) presented statefinders, a pair of dimensionless cosmological parameters that are defined as follows:

$$r=\frac{\dddot{a}}{aH^3},\quad s=\frac{r-1}{3(q-\frac{1}{2})}\tag{26}$$

The statefinder parameters in the model are

$$r=1-2\beta^2\left(tanh^2(\alpha\ t)-1\right)+3\beta\left(coth^2(\alpha\ t)-1\right)\tag{27}$$

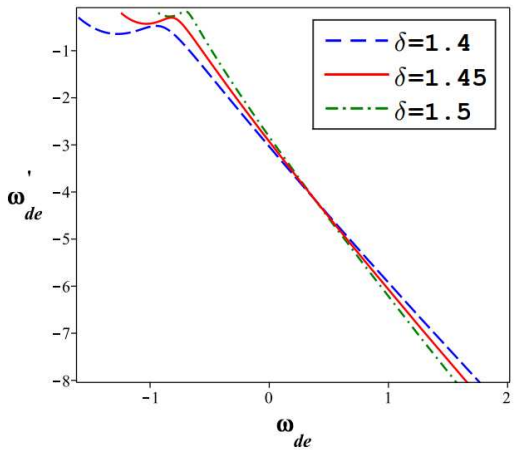

Fig. 6. Plot of $\omega_{de} - \omega'_{de}$ plane for $\beta = 1.5,\ \alpha = 0.11,\ n = 2.3,\ w = 0.0075,\ d = 0.38,\ \delta = 1.5$ and $\varphi_0 = 0.5$.

$$s = \frac{-2\beta^2\left(tanh^2(\alpha\ t) - 1\right) + 3\beta\left(coth^2(\alpha\ t) - 1\right)}{\left(-3\frac{\beta\ (sinh(\alpha\ t))^2}{(cosh(\alpha\ t))^2} + 3\ \beta - 4.5\right)^{-1}} \tag{28}$$

The well-known regions are defined as follows by these statefinders: For (r,s)=(1,0) and (r,s)=(1,1), respectively, ΛCDM and CDM models. The phantom and quintessence DE phases are found in the $s>0$ and $r<1$ regions. The Chaplygin gas model is defined by $r>1$ with $s<0$. We got the statefinders for our model by substituting the average scale factor a(t), Hubble's parameter H(t), and deceleration parameter q(t).

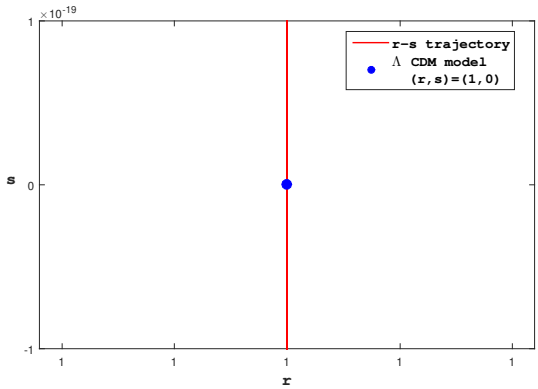

Fig. 7. Plot of statefinders for $k = -1.5$, $c_2 = -0.005$ and $M = 0.125$.

Our model's statefinder plane is depicted in Fig. 7. The statefinder plane's trajectory reaches the ΛCDM limit in its evolution, as can be shown. In its evolution, the r-s trajectory also shows phantom, quintessence, and Chaplygin gas behaviour.

r-q plane:

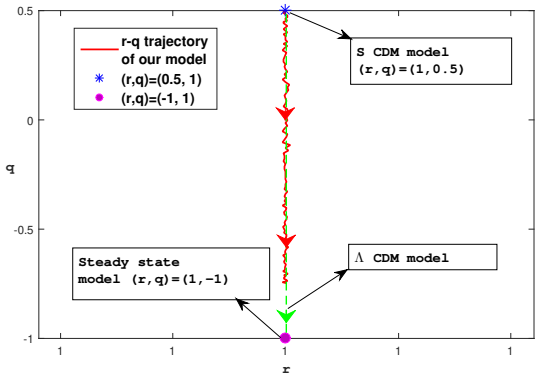

Fig. 8. The evolution of our model in the r-q plane for $k=-1.5$, $c_2=-0.005$ and $M=0.125$.

The behaviour of our DE model on the r-q plane is seen in Fig. 8. The fixed points $(r, q) = (1, 0.5)$ and $(r, q) = (1, -1)$ for standard cold dark matter (SCDM) and Steady State (SS) models, respectively, are shown by the blue and pink colour dots. The time evolution of the ΛCDM model is shown by the dotted line (green colour) at $r = 1$. Our DE model begins with the SCDM model and progresses to the SS model at a later time, as shown by the r-q trajectory. It can also be shown that our model's evolution coincides with that of the ΛCDM model. It's worth noting that the r-q trajectory of our DE model behaves similarly to that of DE models obtained in literature (Singh and Kumar 2016; Dasunaidu et al. 2018a; Prasanthi and Aditya 2020; Aditya et al. 2021).

5 Summary and Conclusions

We studied flat FRW type KK cosmological models in the Saez-Ballester scalar-tensor theory of gravitation in this paper. We have obtained a Tsallis HDE model by solving the field equations using an average scale factor proposed by Mishra et al. (2016). We discovered all the cosmological parameters of our models and examined their relevance to modern cosmology in depth. The following is a summary of our findings:

We notice that the scalar field reduces with cosmic time and we that the SF is decreasing, and that the kinetic energy is increasing as a result. This tendency is quite identical to the scalar field in the dark energy scalar field models

developed by several authors (Jawad et al. 2015; Raju et al. 2019; Bhaskara Rao et al. 2022). The study of the deceleration parameter shows that our model has a smooth transition from the early deceleration epoch to the universe's current acceleration era. The present value of the DP seems to be -0.7324 and our model starts accelerating expansion at 6 Gyr, or 7.7 Gyr ago from today ($t_0 = 13.7$ Gyr). This behaviour is supported by data from a variety of observational schemes $q = -0.930 \pm 0.218$ (BAO + Masers +TDSL+Pantheon+H_z) (Cunha 2009; Li et al. 2011; Amirhashchi and Amirhashchi 2019; Capozziello et al. 2019).

The SEC is observed to be satisfied at the beginning of the period and then violated subsequently. Throughout the evolution of the universe, all other energy conditions are fulfilled. This is attributed to the universe's late-time acceleration, which is supported by current observational data. The EoS parameter begins in the matter-dominated era, evolves to the quintessence DE era, and finally approaches the vacuum DE and phantom era. For $\delta = 1.5$, the EoS parameter becomes -1, i.e., the cosmological constant. This is in agreement with the predictions of Saridakis et al. (2018). For δ =1.45 and 1.5, the model crosses the phantom divided line $\omega_{de} = -1$ and enters the phantom region. The current values of our model's EoS parameters (δ, ω_{de})=(1.4, -1.59), (1.45, -1.24), and (1.5, -0.96) are in good agreement with Planck observational data (Aghanim et al. 2018) $\omega_{de} = -1.56^{+0.60}_{-0.48}$ (Planck + TT + lowE); $\omega_{de} = -1.58^{+0.52}_{-0.41}$ (Planck + TT,TE,EE+lowE); $\omega_{de} = -1.57^{+0.50}_{-0.40}$(Planck + TT,TE,EE+lowE+lensing); $\omega_{de} = -1.04^{+0.10}_{-0.10}$ (Planck + TT,TE,EE+lowE+lensing+BAO).

Study of stability analysis exhibits that our model is stable initially, but the model becomes unstable later on. We have noticed that $\omega_{de} - \omega'_{de}$ plane represents the freezing region throughout the evolution of the universe. This is consistent with recent observations, as the freezing zone has a faster rate of cosmic expansion than the thawing region. The statefinder plane's trajectory reaches the ΛCDM limit in its evolution. In its evolution, the r-s trajectory also shows phantom, quintessence, and Chaplygin gas behaviour. Our Tsallis HDE model begins with the SCDM model and progresses to the SS model at a later time, as shown by the r-q trajectory. It can also be shown that our model's evolution coincides with that of the ΛCDM model. It's worth noting that the r-q trajectory of our DE model behaves similarly to that of DE models obtained in the literature (Singh and Kumar 2016; Dasunaidu et al. 2018a; Prasanthi and Aditya 2020; Aditya et al. 2021).

The study of the models presented here will help to understand DE models in Saez-Ballester theory in the five-dimensional geometry.

Acknowledgements The authors are very much grateful to the reviewer for their constructive comments which certainly improved the presentation of the paper. We are grateful to Prof. D.R.K. Reddy for helpful discussions.

References

Aditya, Y., et al., 2016, *Astrophys. Space Sci*, 361: 56
Aditya, Y., Reddy, DRK., 2018a, *Astrophys Space Sci,* 363: 207
Aditya, Y., Reddy, DRK., 2018b, *Eur. Phys. J. C,* 78: 619
Aditya, Y., Reddy, DRK., 2018c, *Int. J. Geom. Methods Mod.* 15: 1850156.
Aditya, Y., Reddy, DRK., 2019, *Astrophys Space Sci,* 364: 3

Aditya, Y., et al., 2019a, *Results in Physics*, 12: 339.
Aditya, Y., et al., 2019b, *Eur. Phys. J. C,* 79: 1020
Aditya, Y., et al., 2021, *New Astronomy*, 84: 101504.
Aditya, Y., et al., 2023, *Bulg. Astron. J.,* 39: 52
Aditya, Y., 2023, *Bulg. Astron. J.,* 39
Aghanim, N., et al., 2018, A&A, 641: A6
Amirhashchi H, Amirhashchi S., 2019, *Phys Rev D*, 99: 023516
Appelquist T, Chodos A., 1983, *Phys. Rev. Lett*, 50: 141
Bhaskara Rao, MPVV., et al., 2022, New Astronomy, 92: 101733.
Brans C, Dicke RH., 1961, *Phys. Rev*, 124: 925
Caldwell RR, Linder EV., 2005, *Phys Rev Lett*, 95: 141301
Caldwell RR., 2002, *Phys. Lett.B*, 545: 23
Capozziello S, et al., *MNRAS*, 484: 4484
Chiba T, et al., 2000, *Phys. Rev D*, 62: 23511
Chodos A, Detweller S., 1980, *Phys. Rev. D,* 21: 2167.
Cohen, A., et al., 1999, *Phys. Rev. Lett,* 82: 4971
Cunha JV., 2009, *Phys Rev D*, 79: 047301.
Dasunaidu, K et al., 2018a, *Eur. Phys. J. Plus*, 133: 303.
Dasunaidu, K et al., 2018b, *Astrophys Space Sci*, 363: 158.
Deniel Raju, K., et al., 2020, *Can J Phys*, 98: 993-998.
Elizalde E, et al., 2004, *Phys. Rev. D*, 70: 043539
Ghaffari, S., et al., 2019, *Phys. Dark Universe,* 23: 100246
Harko T, et al., 2011, *Phys. Rev. D,* 84: 024020
Iqbal, A., Jawad, A., 2019, *Phys. Dark Universe,* 26: 100349
Jawad, A. et al., 2015, *Commun. Theor. Phys.* 64: 590.
Li, Z, et al., 2011, *Phys Lett B*, 695: 1.
Li, M., 2004, *Phys. Lett. B,* 603: 1
Maity, S., Debnath, U., 2019, *Eur. Phys. J. Plus,* 134: 514
Mishra, R.K., et al., 2016, *Int. J. Theor. Phys*, 55: 1241.
Naidu, K.D., et al., 2021, *Modern Physics Letters A*, 2150054
Naidu, R.L., et al., 2021, *New Astronomy*, 85: 101564.
Nojiri, S, et al., 2005, *Phys. Rev. D*, 71: 063004
Ozel, C et al., 2010, *Adv. Studies Theor. Phys,* 117: 128
Perlmutter, S. et al., 1999, *Astrophysical Journal*, 517: 565-586
Prasanthi, UYD., Aditya, Y., 2020, *Results of Physics*, 17: 103101.
Prasanthi, UYD., Aditya, Y., 2021, *Phys. Dark Universe*, 31: 100782.
Prasanthi, UYD., Aditya, Y., 2019, *Journal of Physics: A conference series*, 1344: 012041.
Raju, K.D., et al., 2019*, Can J Phys*, 97: 932.
Rao, VUM et al., 2018, *Results in Physics,* 10: 469
Rao, VUM, et al., 2012*, Astrophys Space Sci*, 337: 499-501
Rao, VUM, et al., 2015a, *Prespacetime Journal,* 6: 947.
Rao, VUM, et al., 2015b, *The African Review of Physics*, 10: 0060.
Rao, V.S., et al., 2022, *Journal of Dynamical Systems and Geometric Theories*, 20: 227-247.
Ratra B, Peebles PJE., 1988, *Phys. Rev D*, 37: 3406
Ravindranath, P.J., et al., 2018, *Eur. Phys. J. Plus*, 133: 376.
Reddy, DRK et al., 2016, *Astrophys Space Sci* , 361: 356
Riess, AG, et al., 1998, *Astron. J.* 116, 1009-1038
Saez, D, Ballester, VJ., *Physics Letters A*, 113: 467-470
Sahni, V, et al., 2003, *J Exp Theor Phys Lett,* 77: 201
Santhi, MV., et al., 2016a, *Astrophys Space Sci*, 361: 142.
Santhi, MV., et al., 2016b, *Can J Phys*, 94, 578-582.
Santhi, MV., et al., 2017, *Int. J. Theor. Phys.,*56: 362-371.
Santhi, MV., Sobhanbabu, Y., 2020, *Eur. Phys. J. C*, 80: 1198.
Saridakis, EN., et al., 2018, *JCAP,* 12, 012
Sharif, M., Khanum, F., 2011, *Astrophys Space Sci,* 334: 209-214
Singh, CP., Pankaj Kumar., 2016, *Astrophys Space Sci*, 361: 157
Susskind, L., 1995, *J. Math. Phys*, 36: 6377
Tavayef, M., et al., 2018, *Phys. Lett. B*, 781: 195
Tsallis, C., Cirto, LJL, 2013, *Eur. Phys. J. C*, 73: 2487
Witten, E., 1984, *Phys. Lett. B,* 149: 351